

Tuning of Adhesion and Disintegration of Oxidized Starch Adhesives for the Recycling of Medium Density Fiberboard

Muhammad Adly Rahandi Lubis,^a Byung-Dae Park,^{b,*} and Min-Kug Hong^c

Oxidized starch (OS) adhesives with a balance between their adhesion and disintegration properties were prepared by controlling the degree of oxidation and modifying the cross-linker type and level to replace urea-formaldehyde (UF) resins for easy recycling of medium density fiberboard (MDF). Four molar ratios of H₂O₂/starch, two types of cross-linker, *i.e.*, blocked-pMDI (B-pMDI) and citric acid (CA), and three levels of the cross-linkers were employed to tailor the performance of the OS adhesives. The OS reacted with the isocyanate groups from the B-pMDI to form amide linkages, while it formed ester linkages by reacting with the CA. The resulting B-pMDI/OS-bonded MDF had better physical and mechanical properties than the CA/OS-bonded MDF, with comparable adhesion (0.34 MPa) to UF resins and ten times greater degree of fiber disintegration than UF resins. The combination of a 0.5 molar ratio OS with 7.5 wt% of B-pMDI produced MDF exhibiting an optimal balance between adhesion and disintegration, suggesting that such OS adhesives could someday replace UF resins in manufacturing and recycling of MDF without formaldehyde emission.

Keywords: Blocked pMDI; Citric acid; Cross-linking; Oxidized starch adhesives; Medium density fiberboard; Recycling

Contact information: a: Research Center for Biomaterials, Indonesian Institute of Sciences, Cibinong, Bogor, 16911, Indonesia; b: Department of Wood and Paper Science, Kyungpook National University, Daegu, 41566, Republic of Korea; c: Department of Research and Development, Sunchang Corporation, Incheon, 22302, Republic of Korea; *Corresponding author: byungdae@knu.ac.kr

INTRODUCTION

As medium density fiberboard (MDF) production is growing rapidly, waste MDFs are often disposed of using traditional methods such as burning or landfilling, which can harm the environment (Tatàno *et al.* 2009). Recently, advances have been made in the recycling of waste MDFs by converting them into cellulose nanocrystals (Courret *et al.* 2017; Gu *et al.* 2017; Irle *et al.* 2019). However, the process requires several chemical treatments to remove the extractives, hemicelluloses, and lignin before acid hydrolysis, which can increase the cost of recycling. Another means of recycling waste MDFs is to re-manufacture them, which mitigates the impacts on climate change, resources, and human health by ensuring that the carbon remains in the products (Oliveux *et al.* 2015; Morris 2017). However, it is difficult to remove cured urea-formaldehyde (UF) resins from waste MDFs (Grigsby *et al.* 2014; Lubis *et al.* 2018b). The remaining cured resins affect the properties of recycled fibers and recycled MDF (Roffael and Hüster 2012; Hong *et al.* 2018). Moreover, recycling of waste MDFs bonded with UF resins releases formaldehyde, which is toxic. Therefore, the search for alternative adhesives for the manufacture of MDF has become a topic of intensive research. For example, lignin, chitosan, and starch have

been developed as alternative adhesives for MDF (Hoareau *et al.* 2006; Abbott *et al.* 2012; Hubbe *et al.* 2018). Because starch is generally cheaper and easier to isolate than other renewable adhesives, it offers greater potential as an alternative adhesive in such contexts.

Wood adhesives are integral to improving the efficient use of raw materials in the wood-based panel industry and to recycling the panels at the end of their service life (Frihart 2015). Researchers have focused on the development of bio-based adhesives because the most commonly used wood adhesives are synthesized from non-renewable resources and toxic, non-recyclable chemicals (He 2017). Among the renewable adhesives, starch has been used for bonding wood (Onusseit 1992), but the high water-affinity of the hydroxyl (–OH) groups of starch results in poor water resistance, slow setting, and high viscosity of starch-based adhesives (Imam *et al.* 1999; Glavas 2011). Esterification and grafting modifications can increase the water resistance of starch-based adhesives (Wang *et al.* 2011; Zia-ud-Din *et al.* 2017). However, the high viscosities of such modified starch-based adhesives limit their use, particularly in the spraying-blending techniques used in MDF manufacturing. Acceptable viscosities for adhesives used in MDF manufacturing are considered to be between 80 and 300 mPa·s (Park *et al.* 2001; Ji *et al.* 2018). A potential method for decreasing the viscosity of starch to a workable range is oxidation, which depolymerizes starch by breaking α -(1→4)-glucosidic linkages and converts –OH groups into aldehyde (–CHO) and carboxyl (–COOH) groups (Rutenberg and Solarek 1984; Yu *et al.* 2017). Two oxidants are commonly used in the preparation of oxidized starch (OS): sodium hypochlorite and hydrogen peroxide (H₂O₂). Due to environmental issues related to the use of hypochlorite, peroxide oxidation is preferable (Tolvanen *et al.* 2009).

A cross-linker is often used to build a network structure and to accelerate the curing process of OS. Cross-linking can reinforce hydrogen bonds between starch molecules and eventually improve the mechanical strength and thermal stability of the OS (Imam *et al.* 1999; Sridach *et al.* 2013). Common cross-linkers used for OS include malonic acid, citric acid (CA), and other poly-carboxylic acids (Ghosh Dastidar and Netravali 2012; Shen *et al.* 2015). Among these acids, CA is preferable because it has three –COOH groups and could also promote adhesion by forming ester linkages with –OH groups of wood (Umemura and Kawai 2015; Del Menezzi *et al.* 2018). Moreover, a high functionality of polymeric diphenylmethane diisocyanate (pMDI) resin, *i.e.*, blocked pMDI (B-pMDI), facilitates its use as a cross-linker for OS. The B-pMDI releases free –NCO groups after a de-blocking reaction, and then it can react with –CHO, –COOH, or –OH groups of the OS (Wicks and Wicks, Jr. 2001). The B-pMDI should be de-blocked at temperatures less than 100 °C, because the average core temperature in the preparation of wood-based panels during hot-pressing is in the range of 100 °C to 120 °C (Lubis *et al.* 2017). The free –NCO groups react with the OS to form amide or urethane linkages (Blagbrough *et al.* 1986; Stankovich *et al.* 2006). Therefore, OS cross-linked with B-pMDI could potentially be used as a wood adhesive in the manufacture of MDF.

An alternative adhesive should allow both good adhesion and easy disintegration of MDFs for their eventual recycling. Hence, this study aimed to optimize the preparation of OS adhesives with two cross-linkers (*i.e.*, B-pMDI and CA) to achieve a balance between adhesion and disintegration properties to ensure recyclability of OS-bonded MDFs. Four degrees of oxidation (using different H₂O₂/starch molar ratios) and three levels of cross-linker were employed to tailor the performance of the OS adhesives. Properties of the OS adhesives were characterized by several techniques. The adhesion and recyclability of the OS-bonded MDFs were evaluated in detail. The optimum degree of oxidation, cross-linker type, and cross-linker content were obtained using statistical analysis.

EXPERIMENTAL

Materials

Corn starch (28.5% amylose, 18% moisture), hydrogen peroxide (30 wt%) as an oxidizer, copper sulfate (99 wt%) as a catalyst, sodium dodecyl sulfate (98 wt%) as a surfactant, and ammonium persulfate (99 wt%) as an anti-retrogradation agent were used to prepare the OS. Polyvinyl alcohol (PVA, molecular weight: 22,000 g/mol) was used as an adhesion promoter. Liquid pMDI (31% NCO), sodium bisulfate (58.5 wt%), and acetone (99.8 wt%) were used to prepare the B-pMDI (Lubis *et al.* 2017). The B-pMDI and CA (99.9 wt%) were used as cross-linkers. Urea granules (99 wt%), formalin (37 wt%), formic acid (20 wt%), and sodium hydroxide (20 wt%) were used to prepare UF resins as a control adhesive, and ammonium chloride (NH₄Cl, 20 wt%) was used as a hardener for the UF resins. These chemicals were purchased from Duksan Pure Chemicals (Ansan, Korea) and Daejung Chemicals & Metals Co., Ltd. (Siheung, Korea). Virgin wood fibers made of red pine (*Pinus densiflora* Siebold & Zucc., 3% moisture content) were supplied from a commercial MDF mill (Sunchang, Incheon, Korea).

Synthesis of Oxidized Starch

Oxidized starches with different H₂O₂/starch molar ratios were prepared according to the previously published methods with some modifications (Zhang *et al.* 2015b; Lubis and Park 2018a). Briefly, a starch solution was prepared by mixing 200 g of corn starch (1.2345 mol) and 250 mL of distilled water. The solution was sonicated for 30 min at 25 °C and 20 kHz. The solution was then gelatinized at 80 °C for 1 h under continuous stirring at 100 rpm. The temperature was adjusted to 50 °C, after which 0.5% of copper sulfate, 0.5% of ammonium persulfate, and 0.25% of sodium dodecyl sulfate (based on the mass of the starch) were added to the gelatinized starch. Finally, 70.5 g of H₂O₂ (0.6221 mol) was added to obtain OS with an H₂O₂/starch molar ratio of 0.5. The oxidation reaction was performed by maintaining the temperature at 50 °C and a pH of 3 for 5 h under continuous stirring at 500 rpm. Oxidized starches with H₂O₂/starch molar ratios of 1.0, 1.5, and 2.0 were prepared using the same method as OS-0.5.

Preparation of OS Adhesives

The OS was first mixed with 15% PVA (based on the OS solids content) as an adhesion promoter, and the mixture was stirred for 2 h at 80 °C and 500 rpm. Further, two types of OS adhesives were prepared for the MDF panel manufacturing and recycling. The first adhesive was prepared by mixing four different H₂O₂/starch molar ratios of OS and B-pMDI (at levels of 5 wt%, 7.5 wt%, and 10 wt% based on the OS solids content), and the mixture was stirred for 10 min at 80 °C and 300 rpm. The second series of OS adhesives was prepared by adding CA at different levels (5 wt%, 7.5 wt%, and 10 wt% based on the OS solids content) to OS with four different H₂O₂/starch molar ratios, which were also stirred for 10 min at 80 °C and 300 rpm. As a control, UF resin adhesive with a final F/U molar ratio of 1.0 (61.7% solids content, 252 mPa·s viscosity, and 187 s gelation time) was synthesized using an alkaline-acid two-step procedure involving addition and condensation reactions, as reported in the literature (Park and Jeong 2011; Lubis and Park 2018b).

Characterization of OS Adhesives

The aldehyde and carboxyl contents of the OS were measured according to published methods (Smith 1967; Yu *et al.* 2017). To determine the carboxyl content,

approximately 5 g of OS was mixed with 25 mL of 0.1 M HCl for 30 min. The sample was filtered and washed with distilled water. The filtrate was then mixed with 300 mL of distilled water, and the mixture was heated to 90 °C in a water bath for 15 min. The sample was titrated directly with 0.025 M NaOH until a pH of 8.3 was reached. For blank determination, 5 g of starch was evaluated using the same method. The measurements were conducted in triplicate.

The aldehyde content of the OS was used to determine the degree of oxidation (DO) of the OS. Approximately 2 g of the OS was mixed with 100 mL of distilled water and 15 mL of hydroxylamine reagent. The sample was heated to 40 °C in a water bath for 4 h and was then titrated directly to a pH of 3.2 with 0.1 M HCl. Furthermore, approximately 2 g of starch was evaluated using the same method for blank determination. The measurements were conducted in triplicate. The DO of the OS was calculated according to Eqs. 1 and 2 (Zhang *et al.* 2012),

$$DO (\%) = \frac{(C_{\text{NaOH}} \times V_{\text{NaOH}}) - (C_{\text{HCl}} \times V_{\text{HCl}})}{m/162} \times 100\% \quad (1)$$

$$DO_s (\%) = DO - DO_B \quad (2)$$

where C_{NaOH} and C_{HCl} are the concentrations (mol/L) of NaOH and HCl used for titration, respectively; V_{NaOH} and V_{HCl} are the volumes (L) of NaOH and HCl used for titration, respectively; m is the weight (g) of the OS; 162 is the molar mass (g/mol) of the starch monomer ($\text{C}_6\text{H}_{10}\text{O}_5$); DO_s is the DO of a sample; and DO_B is the DO of the blank sample.

Fourier-transform infrared (FTIR) spectroscopy (Frontier, PerkinElmer, Waltham, MA, USA) was performed to qualitatively investigate the functional groups of the OS with different H_2O_2 /starch molar ratios. The OS powder was scanned in the range 4000 to 400 cm^{-1} in KBr pellets with a resolution of 4 cm^{-1} and 32 scans per sample. Furthermore, the functional groups of B-pMDI/OS and CA/OS after heating at 100 °C and 160 °C for 30 min were also investigated using FTIR spectroscopy to understand the curing reaction. The spectrum of each adhesive was normalized using the minimum–maximum normalization method (Wilcox 2014).

To ascertain the formation of aldehyde (–CHO) and carboxyl (–COOH) in the OS, the samples were analyzed using a liquid ^{13}C nuclear magnetic resonance (NMR) spectrometer (Avance III 500, Billerica, MA, USA). The OS powder was dissolved in dimethyl sulfoxide (DMSO)- d_6 at a concentration of 50 mg/mL and heated at 50 °C to form a clear solution. The sample was scanned 4,000 times at 75.45 MHz with 1 s of relaxation time and a 45° pulse, according to the published method (Lian *et al.* 2014).

The molecular weight distribution of the OS samples with different H_2O_2 /starch molar ratios was determined using a gel permeation chromatography (GPC) system (GPC Breeze system, Waters, Milford, MA, USA) with a refractive index detector. The GPC samples were prepared by dissolving 50 mg of OS powder in high-purity distilled water. Prior to injection, samples were filtered through a 0.22- μm membrane filter. Universal calibration was performed using pullulan standards with molecular weights of 6,100 kDa to 642,000 kDa. The analytical condition was set at 30 °C, with a 0.8 mL/min flow rate of sodium nitrate (0.02 N NaNO_3) as the mobile phase.

An X-ray diffractometer (XRD, D/Max-2500, Rigaku Miniflex II, Rigaku, Tokyo, Japan) with a $\text{CuK}\alpha$ radiation source ($\lambda = 0.15406 \text{ nm}$) was used to analyze the crystal structure of the starch before and after oxidation. Prior to analysis, samples were dried in an oven at 105 °C for 3 h and powdered using a grinder. The XRD patterns of native starch

and the OS were obtained by scanning the samples at room temperature in the range of 0° to 50°, with a step of 0.02°/min.

A differential scanning calorimetry (DSC) system (Discovery 25, TA Instruments, New Castle, DE, USA) was used to investigate the peak temperatures of the OS adhesives. Approximately 5 mg samples of liquid OS mixed with different contents of cross-linker were sealed in high-pressure capsule pans and then heated from 30 °C to 200 °C. Differential scanning calorimetry was performed at three different heating rates (2.5 °C/min, 5 °C/min, and 10 °C/min) under a nitrogen flow of 50 mL/min.

Properties of OS Adhesives

The solids contents of the OS adhesives were obtained by drying 2 g of a liquid sample in an oven at 105 °C for 3 h and dividing the oven-dried weight by the initial weight. The viscosity of the OS adhesives was determined using a cone-plate viscometer (DV-II+, Brookfield, Middleboro, MA, USA) with a No. 2 spindle at 60 rpm and 27 °C ± 2 °C. The gelation time of the OS adhesives was measured in boiling water using a gelation time meter (Davis Inotek Instrument, Charlotte, NC, USA). The OS was mixed with 5 wt% B-pMDI based on the OS solids content prior to gelation time measurement. Each experiment was repeated three times.

Preliminary Application in Plywood

Plywood was produced using radiata pine (*Pinus radiata* D. Don) veneers and two sets of OS adhesives. A calculated amount of glue (170 g/m²) was used to produce the three-ply plywood with a target size of 300 mm × 300 mm × 6 mm. The plywood was cold-pressed at 8.8 kPa for 20 min and subsequently hot-pressed at 120 °C and 0.8 MPa for 10 min. The plywood samples were conditioned at 20 °C for 2 d before cutting and testing.

Tensile shear strength (TSS) of the plywood was determined according to a standard procedure (KS F 3101 2016). The TSS values of ten specimens (80 mm × 25 mm × 6 mm) were evaluated using a universal testing machine (H50KS, Hounsfield, Redhill, UK) at a cross-head speed of 2 mm/min and 44,482 N of cell load. Multivariate statistical analysis was conducted to compare the plywood properties, and a Duncan multiple range test at $\alpha = 0.05$ was applied to determine the optimum level of OS molar ratio, which was then used for MDF manufacturing. Statistical analysis was performed using SPSS 17 statistical software (SPSS Inc., Chicago, IL, USA).

Preparation of MDF panel

Laboratory MDFs were prepared using B-pMDI/OS, CA/OS, and UF resins. As a control, two MDF panels with 700 kg/m³ density were manufactured using UF resins according to published methods (Hong *et al.* 2017; Lubis *et al.* 2018a). Briefly, a mixture of 12% UF resin and 1% wax (based on the dried fiber mass) was mixed with 3% of hardener (based on the UF resin solids content). The adhesive was sprayed onto the fibers in a drum-type mechanical blender using an atomization nozzle with a diameter of 1.4 mm. The blended fibers were then used to prepare the fiber mat using a centrifugal air blower. The fiber mat was pre-pressed for 30 s and then hot-pressed at 180 °C using a single-phase pressing schedule of 7.85 MPa for 240 s (20 s/mm) to produce MDF panels (300 mm × 400 mm × 12 mm).

For the evaluation of the OS adhesives, six MDF panels with 700 kg/m³ density were prepared using B-pMDI/OS adhesive with various B-pMDI contents (5 wt%, 7.5 wt%, and 10 wt% based on the OS solids content). Approximately 12% of B-pMDI/OS based on

the fiber dry mass was sprayed onto the fibers in a drum-type mechanical blender using an atomization nozzle. The fibers coated with the OS adhesives were then used to prepare the fiber mat using a centrifugal air blower. The fiber mat was pre-pressed for 30 s and then hot-pressed at 180 °C and 7.85 MPa for 600 s (50 s/mm) using a pre-programmed pressing schedule. By using the same method as that for the B-pMDI/OS samples, six MDF panels were prepared using the CA/OS adhesive with different contents of CA (5 wt%, 7.5 wt%, and 10 wt% based on the OS solids content). The resulting MDFs were conditioned for 2 d at 20 °C and 65% relative humidity prior to cutting and testing.

Determination of MDF Properties

Densities of the MDF panels were 731 kg/m³, 736 kg/m³, and 735 kg/m³ for the 5 wt%, 7.5 wt%, and 10 wt% B-pMDI/OS-bonded MDF. Quite similar densities, 730 kg/m³, 734 kg/m³, and 732 kg/m³, were obtained for MDF panels bonded with 5 wt%, 7.5 wt%, and 10 wt% CA/OS. Physical and mechanical properties of the MDF panels were determined using a standard procedure (KS F 3200 2016). For mechanical properties, ten samples (50 mm × 50 mm × 12 mm) were prepared to determine the internal bonding (IB) strength, and four samples (200 mm × 50 mm × 12 mm) were used to obtain the modulus of rupture (MOR) and modulus of elasticity (MOE). The IB strength, MOR, and MOE of the MDF panels were evaluated using the universal testing machine at cross-head speeds of 2 mm/min, 10 mm/min, and 10 mm/min, respectively. Further, ten samples (50 mm × 50 mm × 12 mm) were soaked for 24 h in water, and then their thicknesses and weights were measured after removing the surface water for the thickness swelling (TS) and water absorption (WA) tests. According to the desiccator method, ten MDF samples (150 mm × 50 mm × 12 mm) were placed in a desiccator for 24 h, and then UV-visible spectrophotometry (Optizen 3220 UV, Mecasys, Daejeon, Korea) was used at a wavelength of 412 nm to determine the formaldehyde emission (FE) values.

Evaluation of MDF Recyclability

MDF panels were cut into block specimens (20 mm × 20 mm × 12 mm). A total of forty-two MDF cubes were prepared from seven different MDF samples using UF resins, B-pMDI/OS (5 wt%, 7.5 wt%, and 10 wt% of B-pMDI based on the OS solids content), and CA/OS (5 wt%, 7.5 wt%, and 10 wt% of CA based on the OS solids content) as the adhesives. These blocks were hydrolyzed under two conditions, at 25 °C for 6 h and 80 °C for 1 h, in triplicate for each type of cross-linker. Information about the mass loss, degree of fiber disintegration, weight gain during hydrolysis, pH of the extract solution, and functional groups of the MDFs after hydrolysis was determined to evaluate the recyclability of the MDFs. The mass loss was calculated by dividing the weight of the MDF block after the hydrolysis by the weight before hydrolysis, while the degree of fiber disintegration was calculated by dividing the dry weight of the MDF block after hydrolysis by the dry weight of the MDF block before hydrolysis. The weight gain was calculated by weighing the MDF block during hydrolysis and dividing the mass of MDF block every 1 h for the hydrolysis at 25 °C and every 10 min for the hydrolysis at 80 °C. The functional groups of the solid residues and the hydrolyzates of the MDF blocks after hydrolysis were detected using FTIR spectroscopy from 400 cm⁻¹ to 4000 cm⁻¹ with a resolution of 4 cm⁻¹ and 32 scans per sample. Hydrolyzate samples were prepared by freeze-drying the extract solution as described previously (Lubis and Park 2018b).

Statistical Analysis

Multivariate analysis was conducted to compare the mean values of the MDF properties at $\alpha = 0.05$. When statistical differences were found, the Duncan multiple range test was applied to determine the optimum levels of B-pMDI and CA in the OS adhesives.

RESULTS AND DISCUSSION

Characteristics of OS

Oxidation causes de-polymerization of starch and introduces aldehyde and carboxyl groups into the OS. The FTIR spectra indicated the presence of C=O of –CHO at 1720 cm^{-1} and –COOH groups at 1600 cm^{-1} only in the OS (Fig. 1a) (Ye *et al.* 2018). This indicated that starch was successfully oxidized by converting the –OH groups on the C-2, C-3, and C-6 positions of the glucose unit to –CHO and –COOH groups using H_2O_2 . The peak at 1640 cm^{-1} in both native starch and OS samples was attributed to the vibration of hydrogen bonded with C=O bonds (Ye *et al.* 2018). Further, the normalized intensity of –CHO and –COOH groups increased as a function of the H_2O_2 /starch molar ratio. This implied that a greater DO was obtained for greater H_2O_2 /starch molar ratios, as shown in Fig. 1b. In peroxide oxidation, the H_2O_2 was split into two OH radicals by Cu^{2+} , which acted as a catalyst. The radical OH groups and catalyst then oxidized the OH of the starch into aldehyde groups and released H_2O . Further, the remaining H_2O_2 converted the aldehyde groups into carboxyl groups (Parovuori *et al.* 1995). Therefore, it was clear that greater H_2O_2 /starch molar ratios led to a greater DO due to the greater amount of H_2O_2 present in the system. The range of DO in this study was in agreement with the literature (Zhang *et al.* 2012).

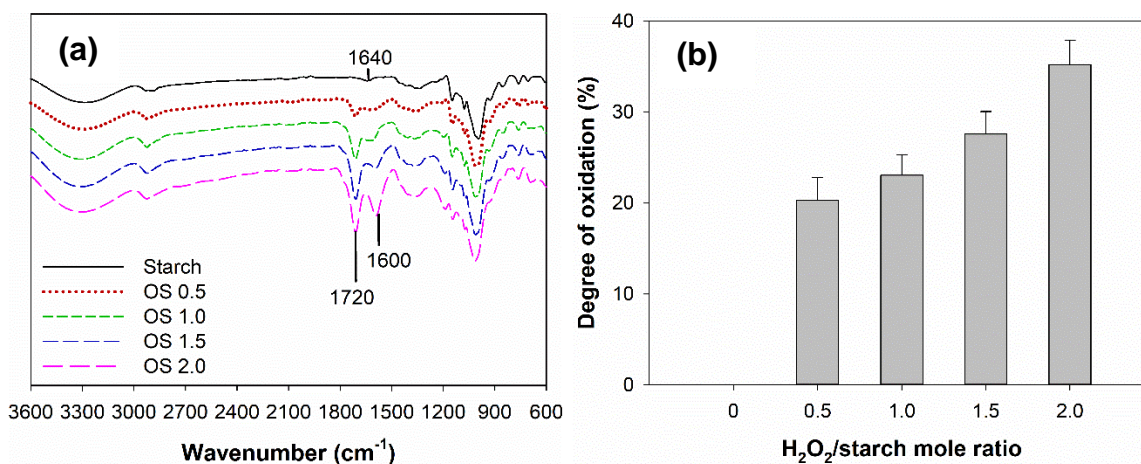


Fig. 1. Characteristics of OS at different H_2O_2 /starch molar ratios: (a) FTIR spectra and (b) DO of the OS

Aldehyde (–CHO) and carboxyl (–COOH) groups in the OS were also detected in the ^{13}C -NMR spectra (Fig. 2a). The chemical shifts of the carbons of native starch were identified at δ 100.7 ppm for C-1; δ 79.2 ppm for C-4; δ 73.8 ppm for C-3, δ 72.4 ppm for C-2, δ 70.0 ppm for C-5; and then δ 60.4 ppm for C-6 (Guo *et al.* 2016; Yu *et al.* 2017). The peak intensities of C-1 and C-4 in the OS decreased when increasing the H_2O_2 /starch molar ratio. This was due to de-polymerization of starch mainly occurring at α -(1→4)-

glucosidic linkages. Furthermore, the peaks of C-2, C-3, and C-6 notably decreased at greater H₂O₂/starch molar ratios, implying oxidation at these positions. Moreover, new peaks of –CHO groups appeared at δ 162.6 ppm and δ 164.5 ppm. However, owing to a high signal-to-noise ratio, a small peak of –COOH groups at δ 175.2 ppm was detected for the OS. This peak only appeared at the greater H₂O₂/starch molar ratio, indicating that –COOH groups were mainly formed *via* conversion of –CHO groups to –COOH groups by the excess H₂O₂ during oxidation (Parovuori *et al.* 1995).

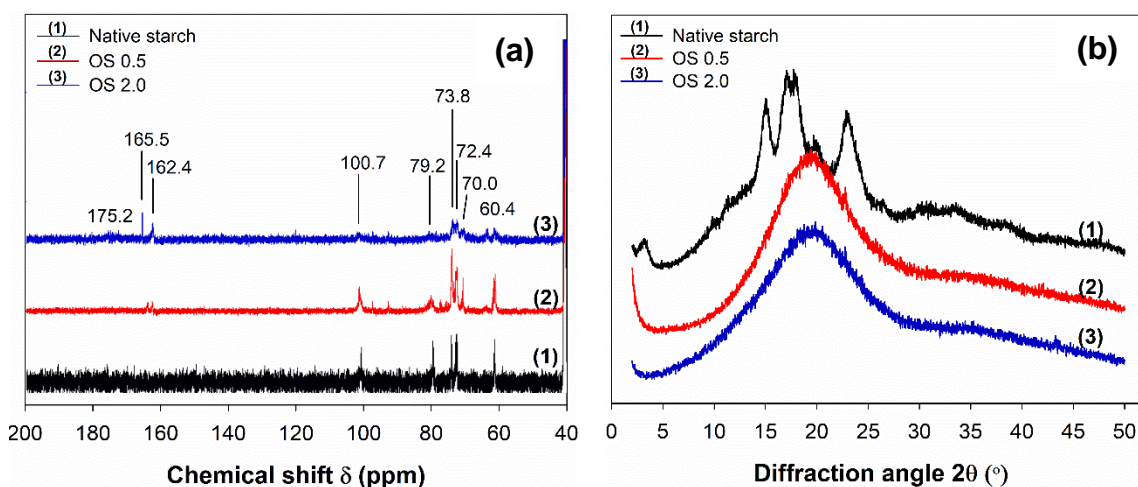


Fig. 2. (a) ¹³C-NMR spectra of OS at different molar ratios and (b) the XRD patterns of OS at different H₂O₂/starch molar ratios

The XRD patterns of the native starch and the OS are presented in Fig. 2b at H₂O₂/starch molar ratios. The X-ray diffractogram of the native corn starch showed peaks at 2θ values of 15.0°, 17.0°, 17.9°, 19.9°, and 22.8°, which indicated that the native corn starch had an A-type crystalline structure (Zhang *et al.* 2009, 2012). However, the oxidation changed the XRD patterns. The crystalline structure became amorphous even at lower H₂O₂/starch molar ratios. The oxidation destroyed the crystalline region of the starch by breaking down the α -(1 \rightarrow 4)-glucosidic linkages, which eventually produced smaller starch molecules. Further, oxidation at greater H₂O₂/starch molar ratios changed the XRD pattern to that of a more amorphous phase.

Functional groups of the B-pMDI/OS and CA/OS adhesives were also evaluated using FTIR spectroscopy after heating at 100 °C for 30 min and at 160 °C for 30 min. As displayed in Fig. 3a, the reaction of OS with B-pMDI or CA at 100 °C for 30 min resulted in a new peak at 1640 cm⁻¹. This peak corresponded to the vibration of hydrogen bonded with C=O of –NCO groups of B-pMDI or –COOH of CA due to the diffusion of molecules toward each other and a phase change of the adhesive from liquid to gel (Upadhyay 2006; Zhang *et al.* 2010). The presence of B-pMDI in the OS was detected by the formation of C=C of aromatic pMDI at 1560 cm⁻¹. In addition, the normalized intensity of C=O of –CHO and –COOH groups at 1720 cm⁻¹ changed with the addition of cross-linkers, but no chemical reaction was observed at this stage. Peaks of around 2924 cm⁻¹ and 3300 cm⁻¹ were detected for C-H and N-H for OS/B-pMDI, and C-H and O-H for OS/CA, respectively. All functional groups in the spectra after heating at 100 °C for 30 min were attributed to the first exothermic peak temperature (T_{p1}) of OS adhesives shown by the DSC (Fig. 6).

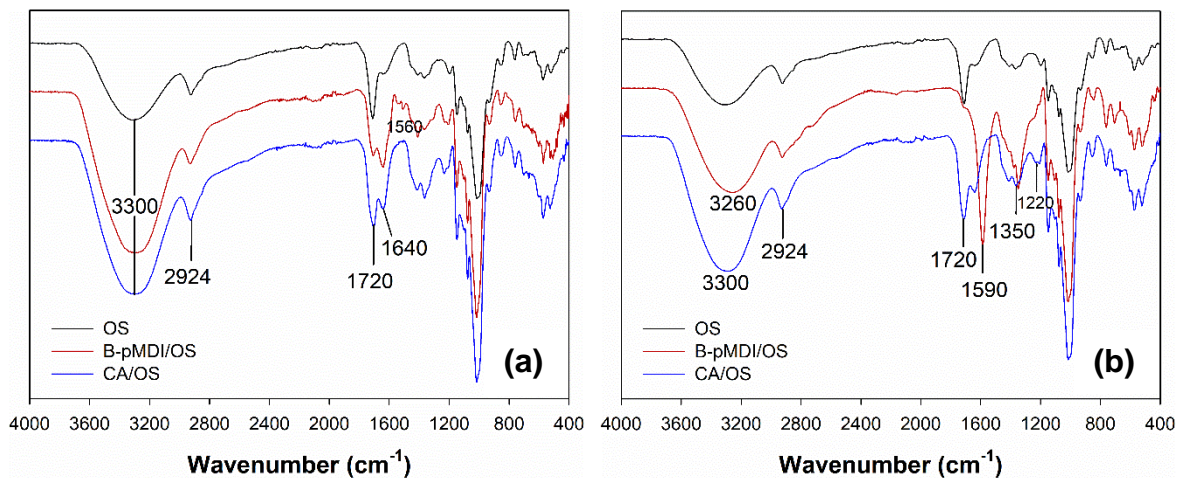


Fig. 3. Typical FTIR spectra of OS-1.0 with 5 wt% cross-linker after heating at (a) 100 °C for 30 min and (b) 160 °C for 30 min

After reacting the OS with the cross-linkers at 160 °C for 30 min (Fig. 3b), B-pMDI/OS produced peaks for C=O of amide linkages at 1590 cm^{-1} and C-N of amide at 1350 cm^{-1} , while CA/OS showed a peak for C=O of ester linkages at 1720 cm^{-1} . Notably, the peaks of C=O of ester and aldehyde groups overlapped at 1720 cm^{-1} . However, a new peak of C-O at 1220 cm^{-1} , which was only detected in the CA/OS, indicated the formation of ester linkages in the CA/OS. This result could be due to the -NCO of B-pMDI reacting with the -COOH of OS to form amide (R-NHCO-O-CO-R) linkages (Blagbrough *et al.* 1986), and the -OH of -COOH of poly-carboxylic acid could have reacted with the -OH or -COOH of OS to form ester (R-COO-R) linkages (Ghosh Dastidar and Netravali 2012). The functional groups in the spectra after heating at 160 °C for 30 min were attributed to the second exothermic peak temperature (T_{p2}) of the OS adhesives shown by the DSC (Fig. 6). The possible cross-linking reactions of the OS adhesives for the two types of cross-linkers are presented in Fig. 4.

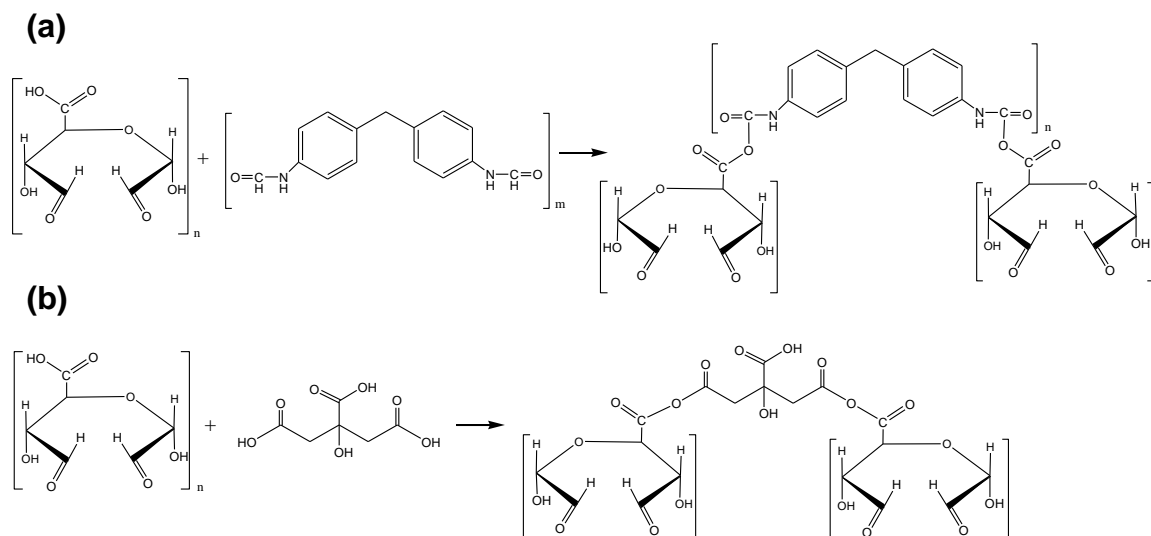


Fig. 4. Possible cross-linking reactions of (a) B-pMDI/OS and (b) CA/OS

Oxidation also affected the solids content, viscosity, and gelation time of the OS adhesives (Table 1). The solids content and viscosity of the OS decreased as the H₂O₂/starch molar ratio increased, while gelation time increased. This result meant that a greater H₂O₂/starch molar ratio decreased the reactivity of the OS adhesive. The excess of H₂O₂ at a greater molar ratio probably remained in the OS, which decreased the solids content and viscosity of the OS and eventually increased the gelation time. Lower viscosity of the adhesive generally increased the gelation time due to the adhesive system needing more time to evaporate the water and solvent. This phenomenon happened to the OS adhesives with greater H₂O₂/starch molar ratios, corresponding to greater amounts of H₂O₂ in the system.

Table 1. Solids Content, Viscosity, Gelation Time, and Molecular Weights of OS for Different H₂O₂/Starch Molar Ratios

Molar Ratio	Solids Content (%)	Viscosity (mPa·s)	Gelation time (s)	M_w (g/mol)	M_n (g/mol)	PDI
0.5	48.4	107.7	532	11,882	9,881	1.19
1.0	41.8	76.0	547	11,000	9,547	1.15
1.5	37.9	60.7	560	9,835	8,890	1.11
2.0	31.2	45.3	587	8,010	7,657	1.05

M_w : weight average molecular weight, M_n : number average molecular weight, PDI: polydispersity index

The molecular weight distributions of the OS for different H₂O₂/starch molar ratios are presented in Table 1. The M_w , M_n , and PDI of the OS decreased as the H₂O₂/starch molar ratio increased. The M_w of the native starch has been reported to be approximately 800,000 g/mol (Zhang *et al.* 2015a), and the M_w decreased by a factor of 100 after oxidation. It was evident that the oxidation de-polymerized the starch macromolecules into smaller molecules and eventually decreased the molecular weight.

Thermal Properties of the OS

The OS adhesives mixed with two different cross-linkers were characterized using DSC; their DSC thermograms are displayed in Fig. 5. As depicted, the exothermic peak temperature (T_p) values of the OS adhesives increased as the heating rate increased. Moreover, two T_p values were detected in both the B-pMDI/OS and CA/OS adhesives. The first T_p (asterisk, T_{p1}) at the lower temperature could be attributed to the diffusion of molecules toward each other and the phase change of the adhesive from liquid to gel (Upadhyay 2006; Zhang *et al.* 2010). The second T_p (arrow, T_{p2}) at greater temperatures could be due to cross-linking between the –OH of OS and –NCO groups of B-pMDI, or –OH of OS with –COOH of CA. At 2.5°/min, OS/B-pMDI and OS/CA had around 79.8 °C of T_{p1} , and the temperature increased to 95.7 °C at 10°/min for OS/B-pMDI and 104.5 °C for OS/CA. Similar trend was observed for T_{p2} of OS/B-pMDI and OS/CA.

As presented in Fig. 5, the B-pMDI/OS generally led to lower T_{p1} values than did the CA/OS, along with lower T_{p2} values than those of the CA/OS, indicating greater reactivity of B-pMDI than that of CA. The T_p values of the OS adhesives decreased as the content of cross-linker increased, indicating that a greater amount of cross-linker accelerated the cross-linking reaction. Greater H₂O₂/starch molar ratios produced lower T_p values than those obtained with lower molar ratios. This result could be due to greater H₂O₂/starch molar ratios providing more carboxyl groups for cross-linking than lower

molar ratios. Regardless of the type of cross-linker, the T_p values of the OS decreased up to a 1.5 H_2O_2 /starch molar ratio and then increased at an H_2O_2 /starch molar ratio of 2.0. This behavior was likely due to the excess of H_2O_2 in OS-2.0 decreasing the OS viscosity markedly by approximately 60% compared to that of OS-0.5, resulting in the OS-2.0 requiring greater temperatures for cross-linking.

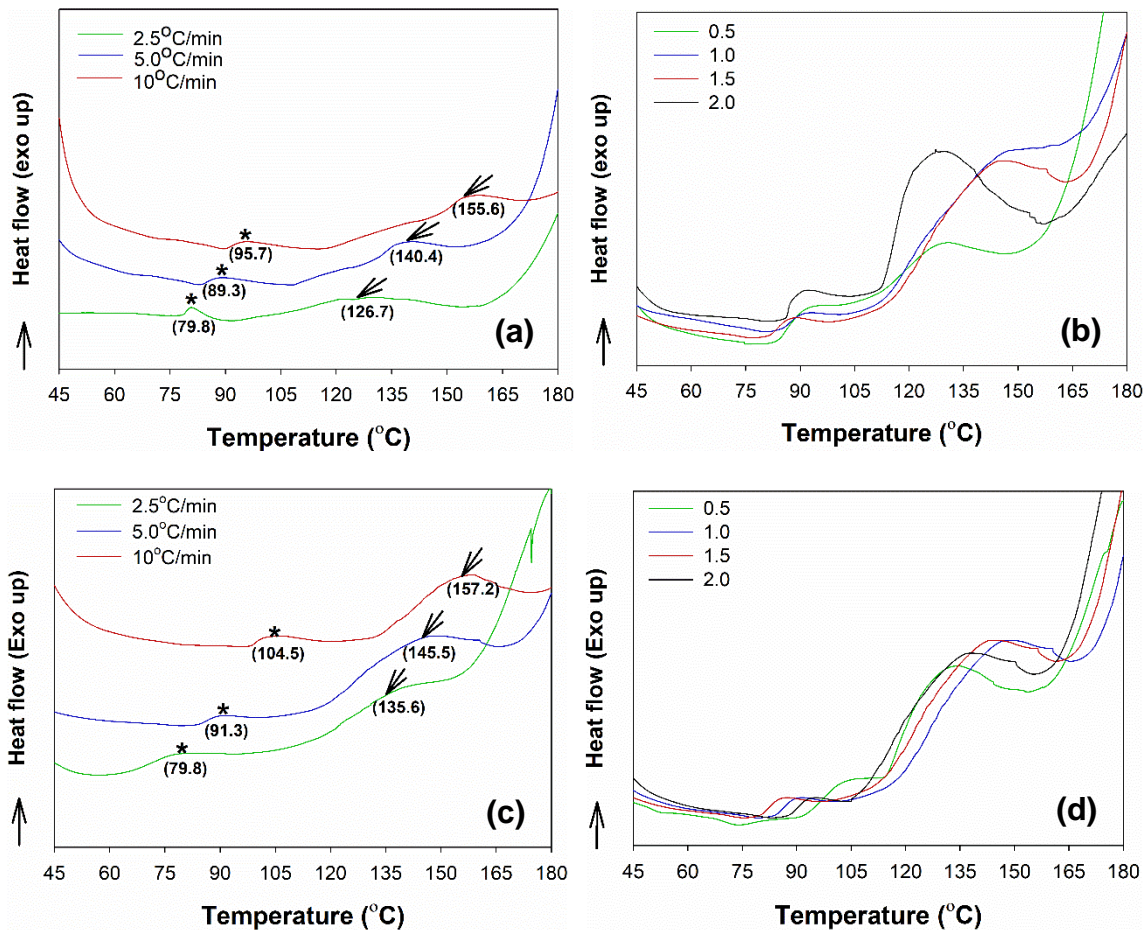


Fig. 5. DSC thermograms of OS adhesives for different H_2O_2 /starch molar ratios and contents of cross-linkers: (a) OS 1.0 with 10 wt% of B-pMDI at different heating rates, (b) OS with different H_2O_2 /starch molar ratios with 10 wt% of B-pMDI at 5 °C/min, (c) OS 1.0 with 10 wt% of CA at different heating rates, and (d) OS with different H_2O_2 /starch molar ratios with 10 wt% of CA at 5 °C/min

Properties of Plywood

The TSS values of the plywood and the statistical analysis results to determine an optimum H_2O_2 /starch molar ratio for the OS are presented in Table 2. As a control, pure OS without added cross-linker was used to prepare plywood panels, but the TSS was only approximately 0.61 MPa, which did not meet the minimum requirement of plywood at 0.70 MPa (KS F 3101 2016). After the addition of cross-linker, the plywood's TSS increased with increasing cross-linker content and was able to meet the minimum requirement of plywood. This result showed that the addition of cross-linker had a significant effect in improving the performance of the OS adhesive by increasing the cross-linking density and forming a bigger network than that without the cross-linker. However, the results also

showed that TSS values decreased as the H₂O₂/starch molar ratio increased. This behavior was probably because the OS adhesive at greater H₂O₂/starch molar ratios had lower solids content and viscosity than those of its counterpart, which eventually increased the gelation time of the OS (Table 1). In addition, a lower viscosity could lead to over-penetration of the OS adhesive into the plywood, leading to poor adhesion strength, as reported for UF-bonded plywood (Nuryawan *et al.* 2014). The results suggested that an H₂O₂/starch molar ratio of 0.5 was optimal for B-pMDI/OS, and an H₂O₂/starch molar ratio of 1.0 was selected for CA/OS. These optimum molar ratios were then used to manufacture MDF panels.

Table 2. Tensile Shear Strength (MPa) of Plywood Bonded with Four Different H₂O₂/Starch Molar Ratios of OS using Different Contents and Types of Cross-linkers

H ₂ O ₂ /Starch Molar Ratio	B-pMDI Level (wt%)			CA Level (wt%)		
	5	7.5	10	5	7.5	10
Control	0.61 (0.06)			0.61 (0.06)		
0.5	0.95 (0.08) ^C	1.13 (0.07) ^B	1.35 (0.10) ^A	0.92 (0.07) ^C	0.96 (0.07) ^C	0.98 (0.05) ^C
1.0	0.96 (0.05) ^C	0.97 (0.07) ^C	0.99 (0.06) ^C	1.01 (0.07) ^C	1.05 (0.08) ^B	1.18 (0.07) ^A
1.5	0.94 (0.10) ^C	0.96 (0.04) ^C	0.98 (0.04) ^C	1.00 (0.08) ^C	1.04 (0.09) ^{BC}	1.08 (0.05) ^B
2.0	0.85 (0.12) ^C	0.92 (0.12) ^C	0.96 (0.12) ^C	0.90 (0.11) ^C	0.92 (0.10) ^C	0.94 (0.10) ^C

Control plywood was prepared using pure OS adhesive without added cross-linker.

Values in the parentheses represent standard deviations.

Values with the same letters are not significantly different at a p-value of 0.05.

Properties of MDF

The IB strengths of MDFs bonded with OS adhesives using different contents and types of cross-linkers are shown in Fig. 6. Many factors affect the IB strength of MDF, such as applied temperature and pressure, moisture content, chemical composition, fiber morphology, and chemical reactions between the adhesive and the fibers (Hubbe *et al.* 2018).

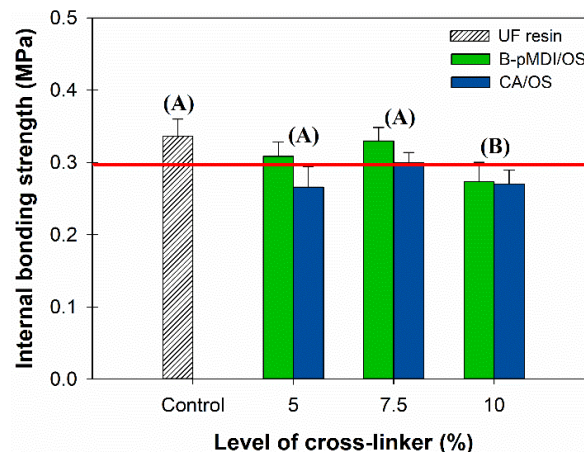


Fig. 6. IB strengths of MDF panels bonded with OS adhesives. The same letters are not significantly different at a p-value of 0.05.

In this study, the B-pMDI/OS-bonded MDF panels generally showed greater IB strengths than did the MDF panels bonded with CA/OS. This result could be due to the amide linkages in B-pMDI/OS giving better overall cross-linking than the ester linkages in CA/OS, leading to better adhesion performance for B-pMDI/OS than for CA/OS. It is known that the $-NCO$ of B-pMDI reacts with the $-COOH$ of OS to form amide (R-NHCO-O-CO-R) linkages (Blagbrough *et al.* 1986), and the $-OH$ of $-COOH$ of poly-carboxylic acid could have reacted with the $-OH$ of $-COOH$ of the OS to form ester (R-COO-R) linkages (Ghosh Dastidar and Netravali 2012; Umemura and Kawai 2015). The IB strengths of the MDF panels bonded with 5 wt% and 7.5 wt% of B-pMDI/OS met the minimum requirement of the standard (0.3 MPa) (KS F 3200 2016), while none of the CA/OS-bonded MDF samples passed the requirement. Statistical analysis showed that the IB strengths of the 5 wt% and 7.5 wt% B-pMDI/OS-bonded MDF samples were not significantly different from that of the UF-bonded MDF.

The results of the MOR testing showed that all of the MDF panels exceeded the minimum standard requirement (15 MPa) (KS F 3200 2016). However, the values were still lower than that of the UF-bonded MDF (Fig. 7a). The MOE values of the MDF samples bonded with OS showed a similar trend to that of the MOR, with the values being lower than that of the UF-bonded panel. The UF-bonded MDF showed a MOE value of approximately 2,809 MPa, while the MDFs bonded with B-pMDI/OS and CA/OS showed MOE values of approximately 2,452 MPa and 2,424 MPa, respectively (Fig. 7b).

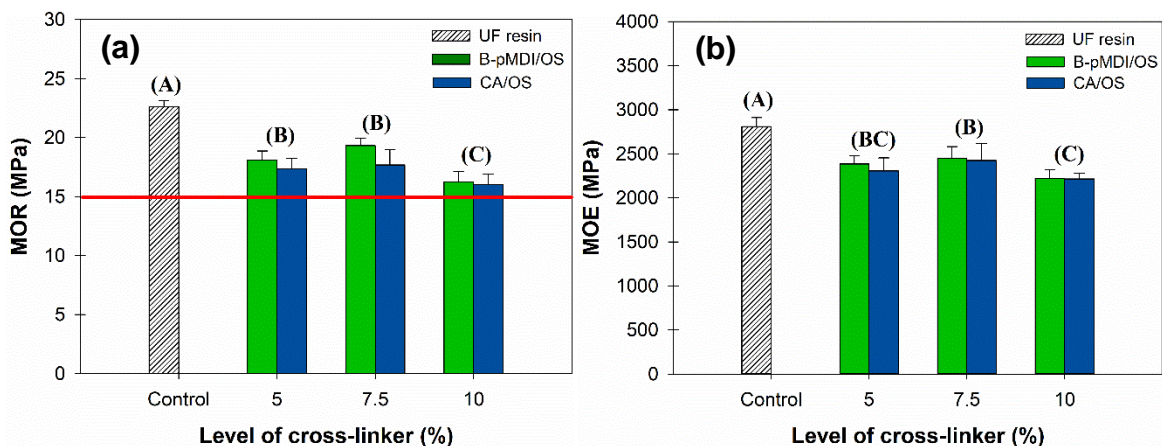


Fig. 7. Mechanical properties of MDF bonded with OS adhesives using different types and contents of cross-linkers: (a) MOR and (b) MOE. The same letters are not significantly different at a p-value of 0.05.

Because formaldehyde was not used in the preparation of the OS adhesives, the FE values were close to the detection limit. Both the B-pMDI/OS- and CA/OS-bonded MDFs showed an average of 0.01 mg/L of FE, while the MDFs bonded with UF resins emitted nearly 90 times this value (Fig. 8). A small amount of formaldehyde from the MDFs bonded with OS adhesives originated from biogenic formaldehyde from lignin components (Tasooji *et al.* 2017). Statistical analysis revealed that 5 wt%, 7.5 wt%, and 10 wt% of a cross-linker in the OS did not significantly influence the FE. This result demonstrated the potential of OS as an alternative to UF resins for the manufacture of MDF that does not produce any FE.

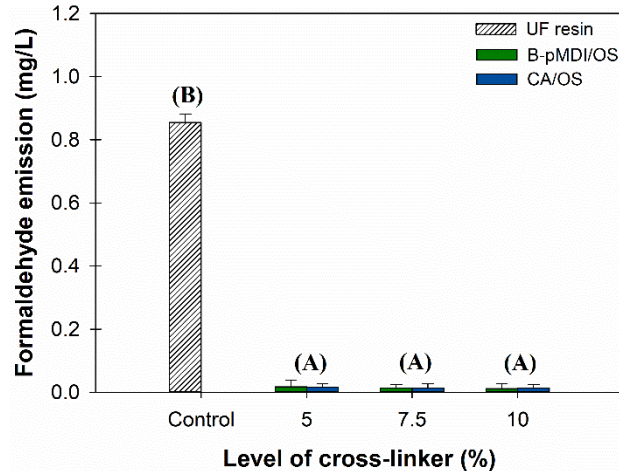


Fig. 8. FE values of MDF bonded with OS adhesives. The same letters are not significantly different at a p-value of 0.05.

The results of the TS and WA tests of the UF-bonded MDF were in agreement with published work (Grigsby *et al.* 2012). However, the TS and WA values of MDFs bonded with OS adhesives were four times higher than those of the UF-bonded MDFs (Fig. 9). When adding cross-linkers, the TS and WA values decreased as the content of cross-linker increased, indicating that the presence of a cross-linker improved the water resistance of the MDF panels. In particular, the TS and WA values of MDF bonded with B-pMDI/OS were lower than for those bonded using CA/OS. The B-pMDI/OS generally improved the water resistance of the MDFs due to the presence of pMDI and effective cross-linking. Therefore, the panel offered notably greater dimensional stability than did the panel bonded with CA/OS. In addition, the CA/OS system can form hydrogen bonds with water molecules through their oxygen atoms, resulting in high solubility of ester linkages in water (Ouellette and Rawn 2018). In contrast, in the absence of acid or base, the hydrolysis of the B-pMDI/OS system through amide linkages in water is slower than that of esters (Boyde 2000; Brown 2000).

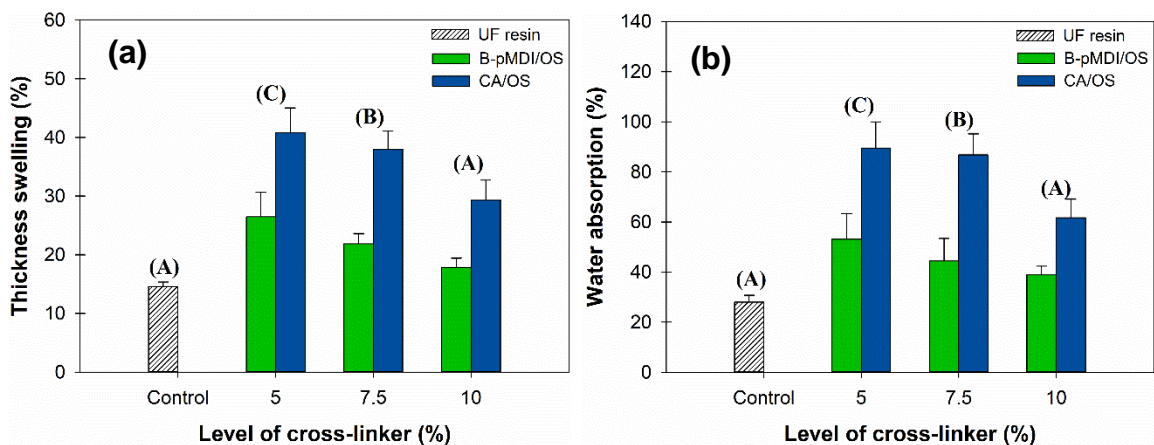


Fig. 9. Properties of MDF bonded with OS adhesives using different types and contents of cross-linkers: (a) TS and (b) WA. Specimens having the same letters are not significantly different at a p-value of 0.05.

Using the results obtained for the physical and mechanical properties of the MDF panels for statistical analysis, the optimum level of cross-linker in the OS was determined to be 7.5 wt% of B-pMDI for a 0.5 molar ratio of OS. At this level, the IB strength of the MDF was comparable to that of UF-bonded MDF, whereas MOR and MOE values were moderately lower. Meanwhile, TS and WA values of the 7.5 wt% B-pMDI/OS-bonded MDF were 10% greater than those of the UF-bonded panel. Obviously, no formaldehyde was detected.

Hydrolysis of MDF

It is necessary to develop OS adhesives that offer a balance between adhesion performance and disintegration for easy recyclability. Here, the recyclability of MDFs bonded with OS adhesives using different contents and types of cross-linkers was investigated under different hydrolysis conditions. The weight gain of MDF panels was evaluated after the hydrolysis of MDF blocks in water at 25 °C for 6 h and 80 °C for 1 h. The results showed that the hydrolysis at 25 °C for 6 h yielded less absorbed water than that at 80 °C for 1 h and thus resulted in lower weight gain during hydrolysis (Fig. 10). High temperature probably causes water molecules to move more quickly, and the molecules are eventually absorbed by the MDF blocks. Regardless of the hydrolysis conditions, the water absorption increased linearly at the beginning and then became slower afterward. The samples approached saturation after an extended time of hydrolysis and eventually reached equilibrium (Muñoz and García-Manrique 2015). In particular, the CA/OS-bonded MDFs absorbed more water than the B-pMDI/OS-bonded MDFs. Regardless of the type of cross-linker, weight gain values decreased as the content of cross-linker increased. Furthermore, the OS-bonded MDFs showed greater weight gain than did the UF-bonded MDFs, showing that the C=O or O-H of the OS-bonded MDFs absorbed more water than those of the UF-bonded MDFs (Guo and Wu 2017; Lubis *et al.* 2019).

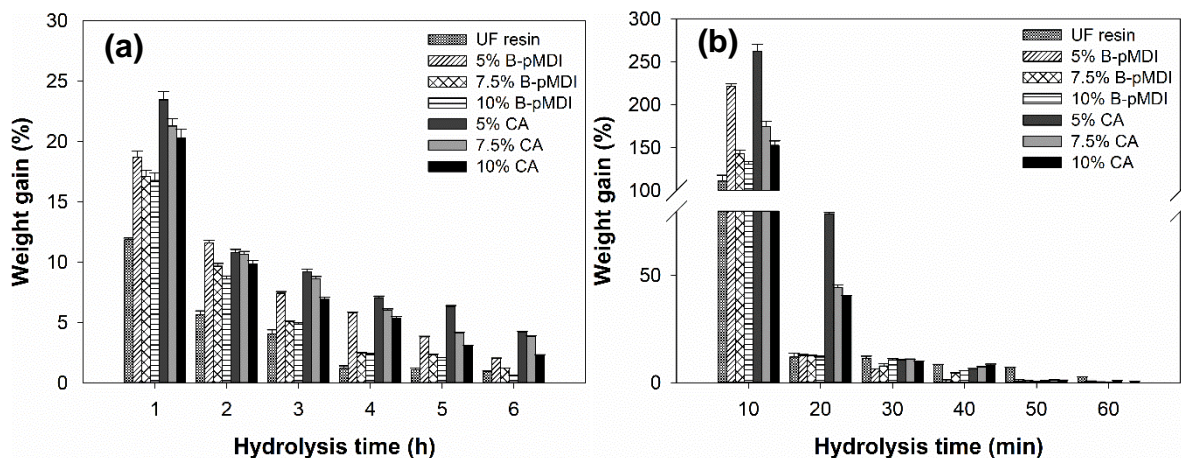


Fig. 10. Weight gain of MDFs during hydrolysis (a) at 25 °C for 6 h and (b) at 80 °C for 1 h

The test results for mass loss and degree of fiber disintegration followed the same trend as that of weight gain (Fig. 11). Due to the greater amount of water absorbed during the hydrolysis at 80 °C for 1 h, the mass loss and degree of fiber disintegration of those MDFs were greater than for those at 25 °C for 6 h. The B-pMDI/OS-bonded MDFs experienced lower mass loss and degree of fiber disintegration than those with CA/OS, indicating that the addition of B-pMDI improved the water resistance of the OS-bonded

MDFs, compared to addition of CA. This result could be because of better cross-linking capacity of B-pMDI/OS through amide linkages, compared to that of CA/OS with ester linkages (Boyde 2000; Brown 2000). In comparison, the UF-bonded MDF showed much greater stability to hydrolysis than the OS-bonded MDFs, indicating that the former was more difficult to recycle (Grigsby *et al.* 2014; Lubis *et al.* 2018b).

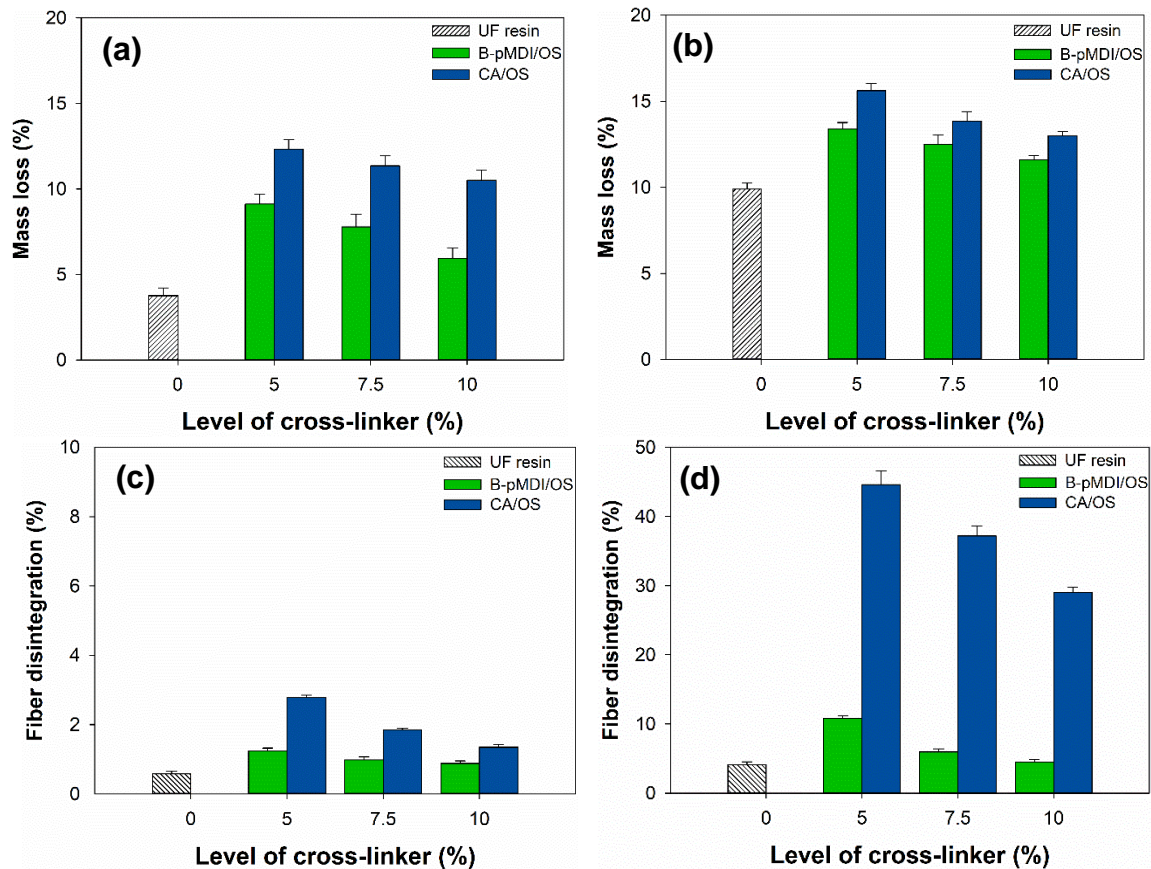


Fig. 11. Recyclability of MDF bonded with OS using different contents and types of cross-linkers: mass loss of MDF after hydrolysis (a) at 25 °C for 6 h and (b) at 80 °C for 1 h; degree of fiber disintegration of MDF after hydrolysis (c) at 25 °C for 6 h and (d) at 80 °C for 1 h

Further investigation was performed to determine the functional groups in the solid residues and hydrolysates of the OS-bonded MDF after hydrolysis. The solid residues of the B-pMDI/OS- and CA/OS-bonded MDFs showed quite similar functional groups after hydrolysis at 25 °C for 6 h and at 80 °C for 1 h (Fig. 12). All residues showed a peak for the C=O of ester groups at 1730 cm^{-1} , due to the reaction of the carboxyl groups of the OS with the -OH of the MDF fibers (Umehura and Kawai 2015). Additional peaks were noted because of the solid residues containing intra-molecular -OH bonds within the MDF fibers (at 1645 cm^{-1}) and the remaining C=O of the aromatic lignin skeleton (at 1600 cm^{-1}) (Müller *et al.* 2009).

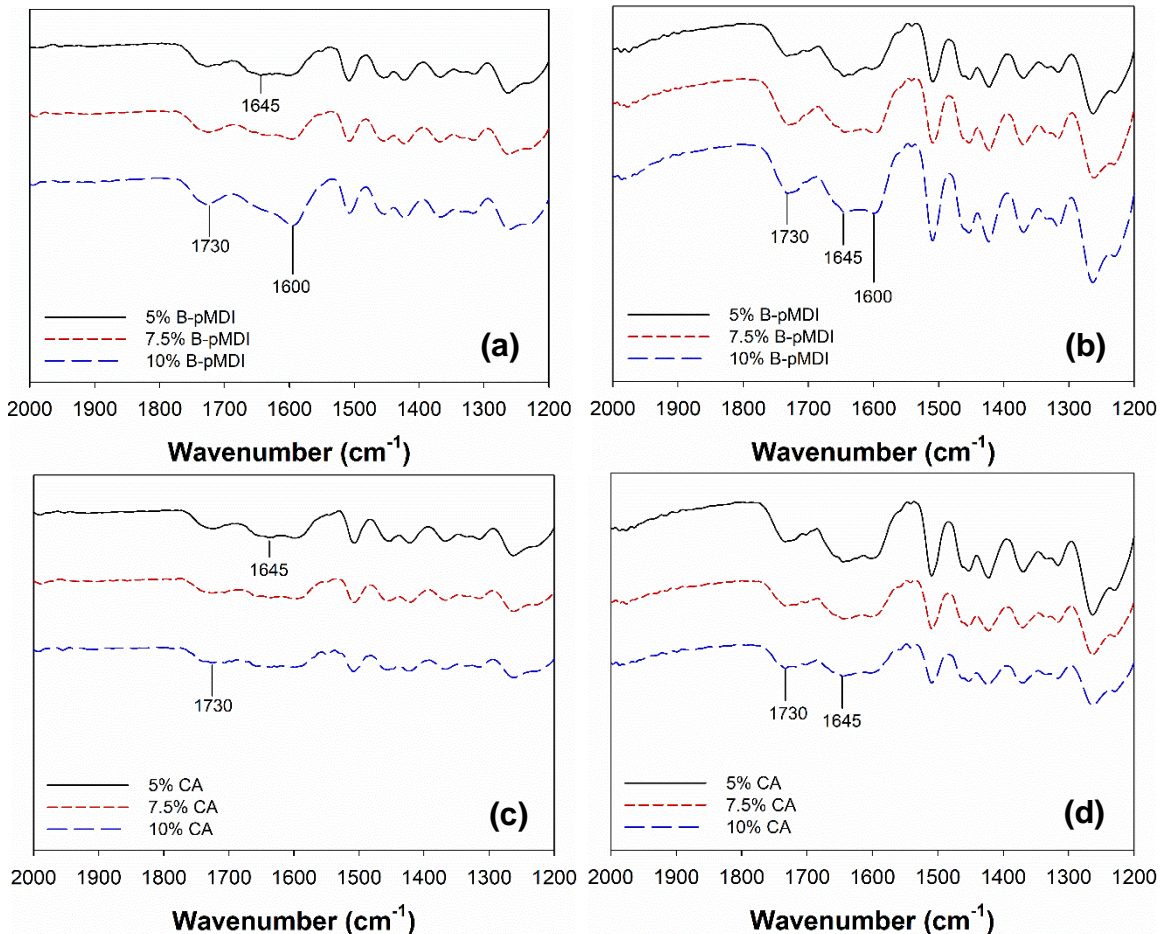


Fig. 12. FTIR spectra of solid residues of MDF bonded with different contents of B-pMDI/OS and CA/OS after hydrolysis: (a) B-pMDI/OS-bonded MDF after hydrolysis at 25 °C for 6 h, (b) B-pMDI/OS-bonded MDF after hydrolysis at 80 °C for 1 h, (c) CA/OS-bonded MDF after hydrolysis at 25 °C for 6 h, and (d) CA/OS-bonded MDF after hydrolysis at 80 °C for 1 h

Different functional groups were detected in the hydrolysates of the B-pMDI/OS- and CA/OS-bonded MDFs (Fig. 13). The C=O of the –CHO group of the OS was clearly detected at 1720 cm^{-1} . This indicated that the –CHO group of the OS did not react with the cross-linker (Fig. 4), and thus the –CHO groups were easily extracted by hydrolysis. However, there was a possibility that the peaks of the C=O of ester linkages and –CHO groups of the CA/OS overlapped at 1720 cm^{-1} because the –COOH of the OS could react with the –OH of the MDF fibers to form ester linkages (Umemura and Kawai 2015; Lubis *et al.* 2019). The –COOH groups showed a peak at 1600 cm^{-1} only after hydrolysis at 80 °C for 1 h. Additional peaks at 1660 cm^{-1} for B-pMDI/OS and 1645 cm^{-1} for CA/OS were attributed to intra-molecular hydrogen bonds of ester or amide bonds in the hydrolysates (Parovuori *et al.* 1995).

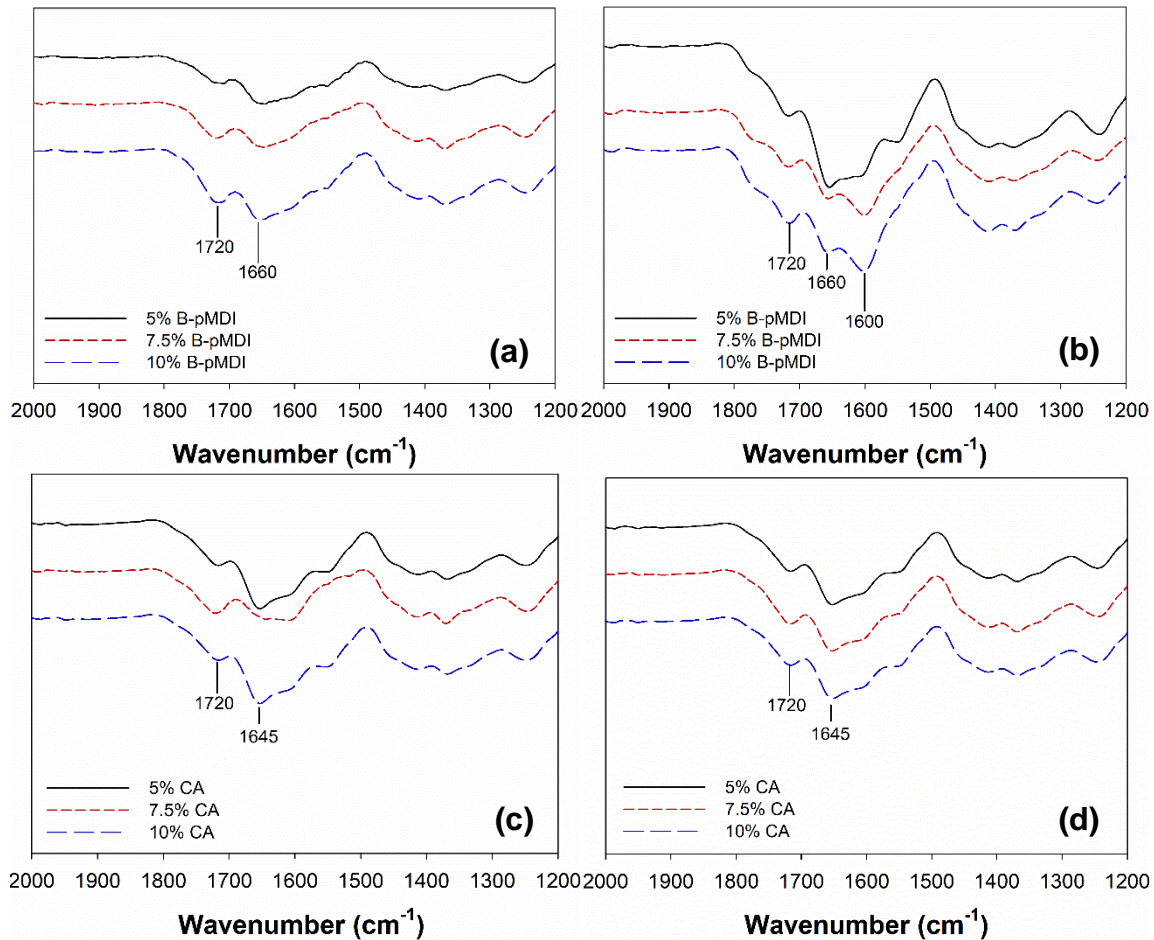


Fig. 13. FTIR spectra of hydrolysates of MDF bonded with different contents of B-pMDI/OS and CA/OS after hydrolysis: (a) B-pMDI/OS-bonded MDF after hydrolysis at 25 °C for 6 h, (b) B-pMDI/OS-bonded MDF after hydrolysis at 80 °C for 1 h, (c) CA/OS-bonded MDF after hydrolysis at 25 °C for 6 h, and (d) CA/OS-bonded MDF after hydrolysis at 80 °C for 1 h

CONCLUSIONS

1. Oxidized starch (OS) adhesives were tailored with various levels of two different cross-linkers to prepare medium density fiberboard (MDF) panels that exhibited a balance between adhesion and disintegration. Addition of B-pMDI as a cross-linker to the OS formed amide linkages, while the combination of citric acid (CA) and OS formed ester linkages.
2. The B-pMDI/OS-bonded MDFs showed better physical properties, mechanical properties, and water resistance than did the CA/OS-bonded MDFs. However, the B-pMDI/OS-bonded MDFs had greater water absorption (WA) and thickness swelling (TS) than did the UF-bonded MDF, which could limit their use.
3. MDF bonded with OS adhesives showed an easy disintegration compared to the urea-formaldehyde (UF)-bonded MDF. A proper level of the B-pMDI and CA in OS adhesives provided a compromise between their adhesion and recyclability of MDF, which was comparable to the UF-bonded MDF.

4. The internal bond (IB) strength of the B-pMDI/OS-bonded MDF was comparable to that of the UF-bonded MDF, though with a much greater degree of disintegration. The results suggested that a 0.5 molar ratio of OS with 7.5 wt% of B-pMDI was the optimum condition to produce MDF with a balance between adhesion and disintegration and could be used as an alternative adhesive to UF resins in the manufacture and recycling of MDF with zero formaldehyde emissions (FE).

ACKNOWLEDGMENTS

This work was supported by the Human Resources Development Project for Big Data-based Global Forest Science 4.0 Professionals (Grant no.: 2019149C10-2023-0301), funded by Korea Forest Service.

REFERENCES CITED

- Abbott, A. P., Palazuela Conde, J., Davis, S. J., and Wise, W. R. (2012). "Starch as a replacement for urea-formaldehyde in medium density fibreboard," *Green Chemistry* 14(11), 3067-3070. DOI: 10.1039/c2gc36194a
- Blagbrough, I. S., Mackenzie, N. E., Ortiz, C., and Scott, A. I. (1986). "The condensation reaction between isocyanates and carboxylic acids. A practical synthesis of substituted amides and anilides," *Tetrahedron Letters* 27(11), 1251-1254. DOI: 10.1016/S0040-4039(00)84230-6
- Boyde, S. (2000). "Hydrolytic stability of synthetic ester lubricants," *Journal of Synthetic Lubrication* 16(4), 297-312. DOI: 10.1002/jsl.3000160403
- Brown, R. S. (2000). "Studies in amide hydrolysis: The acid, base, and water reactions," in: *The Amide Linkage: Structural Significance in Chemistry, Biochemistry, and Materials Science*, A. Greenberg, C. M. Breneman, and J. F. Liebman (eds.), Wiley-Interscience, New York, NY, USA, pp. 85-114.
- Couret, L., Irle, M., Belloncle, C., and Cathala, B. (2017). "Extraction and characterization of cellulose nanocrystals from post-consumer wood fiberboard waste," *Cellulose* 24, 2125-2137. DOI: 10.1007/s10570-017-1252-7
- Del Menezzi, C., Amirou, S., Pizzi, A., Xi, X., and Delmotte, L. (2018). "Reactions with wood carbohydrates and lignin of citric acid as a bond promoter of wood veneer panels," *Polymers* 10(8). DOI: 10.3390/polym10080833
- Frihart, C. R. (2015). "Introduction to special issue: Wood adhesives: Past, present, and future," *Forest Products Journal* 65(1-2), 4-8. DOI: 10.13073/65.1-2.4
- Ghosh Dastidar, T., and Netravali, A. N. (2012). "'Green' crosslinking of native starches with malonic acid and their properties," *Carbohydrate Polymers* 90(4), 1620-1628. DOI: 10.1016/j.carbpol.2012.07.041
- Glavas, L. (2011). *Starch and Protein Based Wood Adhesives*, Master's Thesis, KTH Royal Institute of Technology, Stockholm, Sweden.
- Grigsby, W. J., Carpenter, J. E. P., and Sargent, R. (2014). "Investigating the extent of urea formaldehyde resin cure in medium density fiberboard: Resin extractability and fiber effects," *Journal of Wood Chemistry and Technology* 34(3), 225-238. DOI: 10.1080/02773813.2013.861850
- Grigsby, W., Thumm, A., and Carpenter, J. (2012). "Fundamentals of MDF panel

- dimensional stability: Analysis of MDF high-density layers,” *Journal of Wood Chemistry and Technology* 32(2), 149-164. DOI: 10.1080/02773813.2011.624667
- Gu, J., Hu, C., Zhong, R., Tu, D., Yun, H., Zhang, W., and Leu, S.-Y. (2017). “Isolation of cellulose nanocrystals from medium density fiberboards,” *Carbohydrate Polymers* 167, 70-78. DOI: 10.1016/j.carbpol.2017.02.110
- Guo, J., Lian, X., Kang, H., Gao, K., and Li, L. (2016). “Effects of glutenin in wheat gluten on retrogradation of wheat starch,” *European Food Research and Technology* 242, 1485-1494. DOI: 10.1007/s00217-016-2649-5
- Guo, X., and Wu, Y. (2017). “Characterizing molecular structure of water adsorbed by cellulose nanofiber film using *in situ* micro-FTIR spectroscopy,” *Journal of Wood Chemistry and Technology* 37(5), 383-392. DOI: 10.1080/02773813.2017.1306078
- He, Z. (ed.) (2017). *Bio-based Wood Adhesives: Preparation, Characterization, and Testing*, CRC Press, Boca Raton, FL, USA. DOI: 10.1201/9781315369242
- Hoareau, W., Oliveira, F. B., Grelier, S., Siegmund, B., Frollini, E., and Castellan, A. (2006). “Fiberboards based on sugarcane bagasse lignin and fibers,” *Macromolecular Materials and Engineering* 291(7), 829-839. DOI: 10.1002/mame.200600004
- Hong, M.-K., Lubis, M. A. R., and Park, B.-D. (2017). “Effect of panel density and resin content on properties of medium density fiberboard,” *Journal of the Korean Wood Science and Technology* 45(4), 444-455. DOI: 10.5658/WOOD.2017.45.4.444
- Hong, M.-K., Lubis, M. A. R., Park, B.-D., Sohn, C. H., and Roh, J. (2018). “Effects of surface laminate type and recycled fiber content on properties of three-layer medium density fiberboard,” *Wood Material Science & Engineering*. DOI: 10.1007/s00107-018-1326-8
- Hubbe, M. A., Pizzi, A., Zhang, H., and Halis, R. (2018). “Critical links governing performance of self-binding and natural binders for hot-pressed reconstituted lignocellulosic board without added formaldehyde: A review,” *BioResources* 13(1), 2049-2115. DOI: 10.15376/biores.13.1.Hubbe
- Imam, S. H., Mao, L., Chen, L., and Greene, R. V. (1999). “Wood adhesive from crosslinked poly(vinyl alcohol) and partially gelatinized starch: Preparation and properties,” *Starch* 51(6), 225-229. DOI: 10.1002/(SICI)1521-379X(199906)51:6<225::AID-STAR225>3.0.CO;2-F
- Irle, M., Privat, F., Couret, L., Belloncle, C., Déroubaix, G., Bonnin, E., and Cathala, B. (2019). “Advanced recycling of post-consumer solid wood and MDF,” *Wood Material Science & Engineering* 14(1), 19-23. DOI: 10.1080/17480272.2018.1427144
- Ji, X., Dong, Y., Yu, R., Du, W., Gu, X., and Guo, M. (2018). “Simple production of medium density fiberboards (MDF) reinforced with chitosan,” *Holzforschung* 72(4), 275-281. DOI: 10.1515/hf-2017-0101
- KS F 3101 (2016). “Plywood,” Korean Standards Association, Seoul, Republic of Korea.
- KS F 3200 (2016). “Fiberboards,” Korean Standards Association, Seoul, Republic of Korea.
- Lian, X., Wang, C., Zhang, K., and Li, L. (2014). “The retrogradation properties of glutinous rice and buckwheat starches as observed with FT-IR, ¹³C NMR and DSC,” *International Journal of Biological Macromolecules* 64, 288-293. DOI: 10.1016/j.ijbiomac.2013.12.014
- Lubis, M. A. R., and Park, B.-D. (2018a). “Modification of urea-formaldehyde resin adhesives with oxidized starch using blocked pMDI for plywood,” *Journal of Adhesion Science and Technology* 32(24), 2667-2681. DOI:

- 10.1080/01694243.2018.1511075
- Lubis, M. A. R., and Park, B.-D. (2018b). "Analysis of the hydrolysates from cured and uncured urea-formaldehyde (UF) resins with two F/U mole ratios," *Holzforschung* 72(9), 759-768. DOI: 10.1515/hf-2018-0010
- Lubis, M. A. R., Hong, M.-K., and Park, B.-D. (2018b). "Hydrolytic removal of cured urea-formaldehyde resins in medium-density fiberboard for recycling," *Journal of Wood Chemistry and Technology* 38(1), 1-14. DOI: 10.1080/02773813.2017.1316741
- Lubis, M. A. R., Hong, M.-K., Park, B.-D., and Lee, S.-M. (2018a). "Effects of recycled fiber content on the properties of medium density fiberboard," *European Journal of Wood and Wood Products* 76, 1515-1526. DOI: 10.1007/s00107-018-1326-8
- Lubis, M. A. R., Park, B.-D., and Hong, M.-K. (2019). "Tailoring of oxidized starch's adhesion using crosslinker and adhesion promotor for the recycling of fiberboards," *Journal of Applied Polymer Science* 136(38). DOI: 10.1002/app.47966
- Lubis, M. A. R., Park, B.-D., and Lee, S.-M. (2017). "Modification of urea-formaldehyde resin adhesives with blocked isocyanates using sodium bisulfite," *International Journal of Adhesion and Adhesives* 73, 118-124. DOI:10.1016/j.ijadhadh.2016.12.001
- Morris, J. (2017). "Recycle, bury, or burn wood waste biomass?: LCA answer depends on carbon accounting, emissions controls, displaced fuels, and impact costs," *Journal of Industrial Ecology* 21(4), 844-856. DOI: 10.1111/jiec.12469
- Müller, G., Schöpfer, C., Vos, H., Kharazipour, A., and Polle, A. (2009). "FTIR-ATR spectroscopic analyses of changes in wood properties during particle- and fiberboard production of hard- and softwood trees," *BioResources* 4(1), 49-71. DOI: 10.15376/biores.4.1.49-71
- Muñoz, E., and García-Manrique, J. A. (2015). "Water absorption behaviour and its effect on the mechanical properties of flax fibre reinforced bioepoxy composites," *International Journal of Polymer Science* 2015. DOI: 10.1155/2015/390275
- Nuryawan, A., Park, B.-D., and Singh, A. P. (2014). "Penetration of urea-formaldehyde resins with different formaldehyde/urea mole ratios into softwood tissues," *Wood Science and Technology* 48(5), 889-902. DOI: 10.1007/s00226-014-0649-9
- Oliveux, G., Dandy, L. O., and Leeke, G. A. (2015). "Current status of recycling of fibre reinforced polymers: Review of technologies, reuse and resulting properties," *Progress in Materials Science* 72, 61-99. DOI: 10.1016/j.pmatsci.2015.01.004
- Onusseit, H. (1992). "Starch in industrial adhesives: New developments," *Industrial Crops and Products* 1(2-4), 141-146. DOI: 10.1016/0926-6690(92)90012-K
- Ouellette, R. J., and Rawn, J. D. (2018). "Carboxylic acid derivatives," in: *Organic Chemistry: Structure, Mechanism, and Synthesis (Second Edition)*, Academic Press: London, UK, pp. 665-710. DOI: 10.1016/B978-0-12-812838-1.50022-0
- Park, B.-D., and Jeong, H.-W. (2011). "Hydrolytic stability and crystallinity of cured urea-formaldehyde resin adhesives with different formaldehyde/urea mole ratios," *International Journal of Adhesion and Adhesives* 31(6), 524-529. DOI: 10.1016/j.ijadhadh.2011.05.001
- Park, B.-D., Riedl, B., Hsu, E. W., and Shields, J. (2001). "Application of cure-accelerated phenol-formaldehyde (PF) adhesives for three-layer medium density fiberboard (MDF) manufacture," *Wood Science and Technology* 35, 311-323. DOI: 10.1007/s002260100095
- Parovuori, P., Hamunen, A., Forssell, P., Autio, K., and Poutanen, K. (1995). "Oxidation of potato starch by hydrogen peroxide," *Starch* 47(1), 19-23. DOI: 10.1002/star.19950470106

- Roffael, E., and Hüster, H.-G. (2012). "Complex chemical interactions on thermo hydrolytic degradation of urea formaldehyde resins (UF-resins) in recycling UF-bonded boards," *European Journal of Wood and Wood Products* 70, 401-405. DOI: 10.1007/s00107-011-0574-7
- Rutenberg, M. W., and Solarek, D. (1984). "Starch derivatives: Production and uses," in: *Starch: Chemistry and Technology (Second Edition)*, R. L. Whistler, J. N. Bemiller, and E. F. Paschall (eds.), Academic Press, San Diego, CA, USA, pp. 311-388. DOI: 10.1016/B978-0-12-746270-7.50016-1
- Shen, L., Xu, H., Kong, L., and Yang, Y. (2015). "Non-toxic crosslinking of starch using polycarboxylic acids: Kinetic study and quantitative correlation of mechanical properties and crosslinking degrees," *Journal of Polymers and the Environment* 23(4), 588-594. DOI: 10.1007/s10924-015-0738-3
- Smith, R. J. (1967). "Characterization and analysis of starches," in: *Starch: Chemistry and Technology (Vol. II)*, R. L. Whistler and E. F. Pachall (eds.), Academic Press, New York, NY, USA, pp. 620-625.
- Sridach, W., Jonjankiat, S., and Wittaya, T. (2013). "Effect of citric acid, PVOH, and starch ratio on the properties of cross-linked poly(vinyl alcohol)/starch adhesives," *Journal of Adhesion Science and Technology* 27(15), 1727-1738. DOI: 10.1080/01694243.2012.753394
- Stankovich, S., Piner, R. D., Nguyen, S. T., and Ruoff, R. S. (2006). "Synthesis and exfoliation of isocyanate-treated graphene oxide nanoplatelets," *Carbon* 44(15), 3342-3347. DOI: 10.1016/j.carbon.2006.06.004
- Tasooji, M., Wan, G., Lewis, G., Wise, H., and Frazier, C. E. (2017). "Biogenic formaldehyde: Content and heat generation in the wood of three tree species," *ACS Sustainable Chemistry & Engineering* 5(5), 4243-4248. DOI: 10.1021/acssuschemeng.7b00240
- Tatàno, F., Barbadoro, L., Mangani, G., Pretelli, S., Tombari, L., and Mangani, F. (2009). "Furniture wood wastes: Experimental property characterisation and burning tests," *Waste Management* 29(10), 2656-2665. DOI: 10.1016/j.wasman.2009.06.012
- Tolvanen, P., Mäki-Arvela, P., Sorokin, A. B., Salmi, T., and Murzin, D. Y. (2009). "Kinetics of starch oxidation using hydrogen peroxide as an environmentally friendly oxidant and an iron complex as a catalyst," *Chemical Engineering Journal* 154(1-3), 52-59. DOI: 10.1016/j.cej.2009.02.001
- Umemura, K., and Kawai, S. (2015). "Development of wood-based materials bonded with citric acid," *Forest Products Journal* 65(1-2), 38-42. DOI: 10.13073/FPJ-D-14-00036
- Upadhyay, S. K. (2006). "Reactions in solutions," in: *Chemical Kinetics and Reaction Dynamics*, Springer, New York, NY, USA, pp. 185-203. DOI: 10.1007/978-1-4020-4547-9_8
- Wang, Z., Gu, Z., Hong, Y., Cheng, L., and Li, Z. (2011). "Bonding strength and water resistance of starch-based wood adhesive improved by silica nanoparticles," *Carbohydrate Polymers* 86(1), 72-76. DOI: 10.1016/j.carbpol.2011.04.003
- Wicks, D. A., and Wicks, Jr., Z. W. (2001). "Blocked isocyanates III: Part B: Uses and applications of blocked isocyanates," *Progress in Organic Coatings* 41(1-3), 1-83. DOI: 10.1016/S0300-9440(00)00164-8
- Wilcox, K. E. (2014). *Using Regression Analyses for the Determination of Protein Structure from FTIR Spectra*, Ph.D. Thesis, Univeristy of Manchester, Manchester, UK.

- Ye, P., An, J., Zhang, G., Wang, L., Wang, P., and Xie, Y. (2018). "Preparation of particleboard using dialdehyde starch and corn stalk," *BioResources* 13(4), 8930-8942. DOI: 10.15376/biores.13.4.8930-8942
- Yu, Y., Wang, Y.-n., Ding, W., Zhou, J., and Shi, B. (2017). "Preparation of highly-oxidized starch using hydrogen peroxide and its application as a novel ligand for zirconium tanning of leather," *Carbohydrate Polymers* 174, 823-829. DOI: 10.1016/j.carbpol.2017.06.114
- Zhang, C., Hu, J., Chen, S., and Ji, F. (2010). "Theoretical study of hydrogen bonding interactions on MDI-based polyurethane," *Journal of Molecular Modeling* 16, 1391-1399. DOI: 10.1007/s00894-010-0645-4
- Zhang, S.-D., Zhang, Y.-R., Wang, X.-L., and Wang, Y.-Z. (2009). "High carbonyl content oxidized starch prepared by hydrogen peroxide and its thermoplastic application," *Starch* 61(11), 646-655. DOI: 10.1002/star.200900130
- Zhang, S., Liu, F., Peng, H., Peng, X., Jiang, S., and Wang, J. (2015a). "Preparation of novel c-6 position carboxyl corn starch by a green method and its application in flame retardance of epoxy resin," *Industrial & Engineering Chemistry Research* 54(48), 11944-11952. DOI: 10.1021/acs.iecr.5b03266
- Zhang, Y., Ding, L., Gu, J., Tan, H., and Zhu, L. (2015b). "Preparation and properties of a starch-based wood adhesive with high bonding strength and water resistance," *Carbohydrate Polymers* 115, 32-57. DOI: 10.1016/j.carbpol.2014.08.063
- Zhang, Y.-R., Wang, X.-L., Zhao, G.-M., and Wang, Y.-Z. (2012). "Preparation and properties of oxidized starch with high degree of oxidation," *Carbohydrate Polymers* 87(4), 2554-2562. DOI: 10.1016/j.carbpol.2011.11.036
- Zia-ud-Din, Xiong, H., Wang, Z., Fei, P., Ullah, I., Javaid, A. B., Wang, Y., Jin, W., and Chen, L. (2017). "Effects of sucrose fatty acid esters on the stability and bonding performance of high amylose starch-based wood adhesive," *International Journal of Biological Macromolecules* 104, 846-853. DOI: 10.1016/j.ijbiomac.2017.06.090

Article submitted: December 30, 2019; Peer review completed: April 25, 2020; Revised version received and accepted: May 10, 2020; Published: May 15, 2020.

DOI: 10.15376/biores.15.3.5156-5178